Study of ^{20}Ne(p, t)^{18}Ne transitions with the coupled-channel Born approximation*

David K. Olsen† and Takeshi Udagawa
Center for Nuclear Studies, University of Texas, Austin, Texas 78712

Ronald E. Brown
John H. Williams Laboratory of Nuclear Physics, University of Minnesota, Minneapolis, Minnesota 55455
(Received 5 December 1974)

Differential cross sections have been measured at a proton bombarding energy of 39.8 MeV for ^{20}Ne(p, t) transitions to the 0_1^+, 2_1^+, and 4_1^+ states of ^{18}Ne at 0.0, 1.89, and 3.38 MeV, respectively, and to the $(0_2^+, 2_2^+)$ doublet in ^{18}Ne at (3.58, 3.62) MeV. These cross sections are compared with zero-range coupled-channel Born-approximation calculations in which the coexistence-model wave functions of Benson and Flowers have been used. The inclusion of inelastic effects improves the agreement between experiment and theory; however, the calculated (p, t) cross sections are quite sensitive to the nature of the inelastic processes in the t + ^{18}Ne channel, and, until these processes are better understood, it is not possible for the calculation to provide a sensitive test of the mass-18 nuclear wave functions used.

[NUCLEAR REACTIONS ^{20}Ne(p, t), E = 39.8 MeV; measured $\sigma(\theta)$ and calculated $\sigma(\theta)$ with CCBA and DWBA.]

I. INTRODUCTION

The mass-18 isobars are of particular interest because they are only two nucleons removed from the ^{16}O doubly closed shell and are also only two nucleons removed from ^{20}Ne, whose low-lying states are understood as being members of rotational bands. Because of this, they have been extensively investigated both experimentally and theoretically.[1] The numerous low-lying positive-parity levels and large $B(E2)$ enhancements for these nuclei indicate that the simple shell-model picture of two nucleons moving in the $2s_{1/2}$, $1d_{3/2}$, and $1d_{5/2}$ orbits is not adequate. Therefore, calculations for mass 18 have been reported in which deformed four-particle–two-hole components have been mixed with the usual two-particle states.[2-4] In particular, Benson and Flowers[3,4] have constructed such deformed components by coupling two holes moving in the $1p_{1/2}$ and $1p_{3/2}$ orbits to the members of the ^{20}Ne ground-state rotational band. These coexistence-model calculations[3,4] provide additional energy levels and fit the electromagnetic matrix elements of ^{18}O and ^{18}F remarkably well.

In addition, two-particle-transfer cross sections depend coherently on the configurations of the initial and final states and might provide good tests of the mass-18 wave functions. For example, (t,p) transitions connect T_z = 1, T = 1, mass-18 states to a spherical ^{16}O target, whereas (p, t) transitions connect T_z = −1, T = 1, mass-18 states to a deformed ^{20}Ne target. Distorted-wave–Born-approximation (DWBA) calculations using coexistence-model wave functions reproduce both the shape and magnitude of ^{16}O(t, p)^{18}O cross sections reasonably well.[5] For the ^{20}Ne(p, t)^{18}Ne reaction, however, this is not the case.[6,7] In particular, the shape of the cross section to the first 2^+ state cannot be reproduced with reasonable optical-model parameters, and the calculated relative strength of the first 4^+ state is much smaller than is measured experimentally.

In this paper we report the measurement of ^{20}Ne(p, t)^{18}Ne differential cross sections at 39.8 MeV for transitions leading to the 0_1^+ ground state, the 2_1^+ state at 1.89 MeV, the 4_1^+ state at 3.38 MeV, and the $(0_2^+, 2_2^+)$ doublet at (3.58, 3.62) MeV. These cross-section measurements verify those reported by others[6-9] and are compared here with coupled-channel–Born-approximation (CCBA) calculations.

The CCBA[10] takes into account explicitly inelastic excitations in the entrance and exit channels and allows (p, t) transitions to take place from excited state to excited state in parallel with the normal DWBA-like transition. Effects of the inelastic excitations are expected to be strong where highly collective nuclear states are involved. In particular, it has been shown that CCBA, rather than DWBA, calculations are required to explain experimental (p, t) cross sections for transitions to rotational bands in rare-earth nuclei[11] and for both allowed and forbidden transitions to members of ^{20}Ne rotational bands.[12] These calculations have primarily served to clarify the reaction mechanisms involved in the transi-

tions. In addition, the CCBA has explained[13] many features of (p,t) cross sections connecting vibrational states.

The CCBA calculations for ^{20}Ne$(p,t)^{18}$Ne transitions reported[14] in this paper require microscopic wave functions for ^{20}Ne and ^{18}Ne and a macroscopic coupled-channel description of the inelastic scattering in both the entrance and exit channel. The microscopic coexistence-model wave functions of Benson and Flowers are used.[3,4] These assume the ^{20}Ne ground-state rotational band to be four particles moving in deformed orbits which are determined by minimizing the total energy of the rotational states. Furthermore, data for proton inelastic scattering from ^{20}Ne leading to the first 0^+, 2^+, and 4^+ states are well reproduced with macroscopic coupled-channel calculations using a rotational coupling scheme.[15,16] However, for ^{18}Ne pure rotational coupling to the low-lying states may not be valid. The ^{18}Ne microscopic wave functions contain both spherical and deformed components, thereby allowing nonzero quadrupole moments smaller than the rotational value. In addition, the available inelastic scattering data are ambiguous about the macroscopic description of the low-lying states of the $T=1$, mass-18 nuclei.[17,18] Because of this, CCBA calculations are reported here for both rotational and vibrational coupling schemes for the inelastic scattering in the $t+^{18}$Ne channel. In these calculations the deformations describing the coupling between ^{18}Ne states were obtained from an analysis of cross sections[17] for inelastic scattering of 24.5-MeV protons by ^{18}O.

We find that the inclusion of inelastic effects greatly improves the agreement between calculated and experimental (p,t) cross sections; unfortunately however, the calculated results depend very strongly on the coupling scheme and deformation parameters used to describe triton scattering by ^{18}Ne. These parameters are not well known; therefore, at the present time a comparison of these calculations with experimental cross sections does not provide a very rigorous test of mass-18 coexistence-model wave functions.

II. EXPERIMENTAL APPARATUS, PROCEDURE, AND RESULTS

A 39.8-MeV proton beam from the University of Minnesota proton linear accelerator was focussed onto 99.9% isotopically pure ^{20}Ne gas contained at a pressure of $\frac{1}{3}$ atmosphere in a 10.2-cm-diam gas cell covered with 25.4-μm Havar foil. The charged-particle reaction products were momentum analyzed by a double-focussing 1.0-m radius magnetic spectrometer and were detected by a focal-plane array of 32 surface-barrier 1000-μm detectors. Additional experimental details can be found in Refs. 12 and 19.

Figure 1 shows a triton spectrum obtained at 15° with an energy resolution of about 100 keV. The ^{18}Ne 0_1^+ ground state and the 2_1^+ first excited state are populated strongly. At about twice the energy of the 2_1^+ state a 0_2^+-2_2^+-4_1^+ vibrational-like triplet is excited. The 0_2^+ and 2_2^+ members of this triplet are separated by only 40 keV and have yet to be resolved in (p,t) work.[6-9] The 5.14-MeV group is a doublet above which only a few other states are found to be populated from (p,t) reactions.[6-9] In this work we will only be concerned with the cross sections to the 0_1^+, 2_1^+, 4_1^+, 0_2^+, and 2_2^+ states.

Figure 2 shows differential cross sections to the 0_1^+ ground state and 2_1^+ and 4_1^+ excited states; the curves represent DWBA calculations to be discussed later. Much of the data have relative errors of ±4%, which are about the size of the plotted points. At very small cross sections the relative errors are much larger than this. In addition the absolute cross-section scale has a standard deviation of ±5%. Our measured cross section to the ^{18}Ne 0_1^+ ground state at the first maximum near 30° is 747 μb/sr. Others have measured this (p,t) cross section to be between 650 and 750 μb/sr at the following proton beam energies: 42.6 MeV,[6] 45.0 MeV,[8,9] and 50.0 MeV.[7]

Figure 3 shows the cross section to the unresolved 0_2^+ and 2_2^+ states; the curves will be discussed later. The Rutherford-Laboratory group[7] has estimated the separate 0_2^+ and 2_2^+ contributions to their 50-MeV cross section to this doublet by fitting it using the 0_1^+ ground-state and 2_1^+ excited-state cross sections as standard shapes. They estimate the 0_2^+ strength to be about 0.11 of the 0_1^+

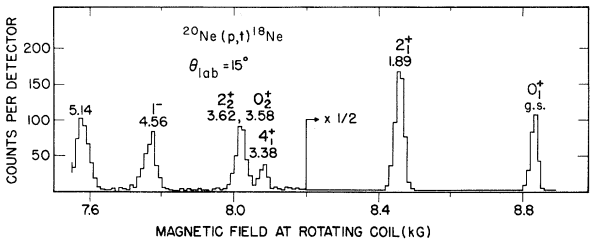

FIG. 1. Triton spectrum at 15° produced by 39.8-MeV proton bombardment of ^{20}Ne. The energy resolution is about 100 keV. The measured cross sections to the 0_1^+ ground state and to the 2_1^+ and 4_1^+ states are shown in Fig. 2, and the measured cross section to the 0_2^+-2_2^+ doublet is shown in Fig. 3.

strength and the 2_2^+ strength to be roughly 0.12 of the 2_1^+ strength. A similar analysis of our 40-MeV doublet cross section gives the 0^+ ratio to be 0.05 and the 2^+ ratio to be 0.35, but at neither energy is the shape of the doublet cross section reproduced well by such an analysis. In any case, the measured doublet cross section provides an upper limit to the sum of the 0_2^+ and 2_2^+ strengths, and the above analyses indicate that both states provide significant contributions to the measured doublet cross section.

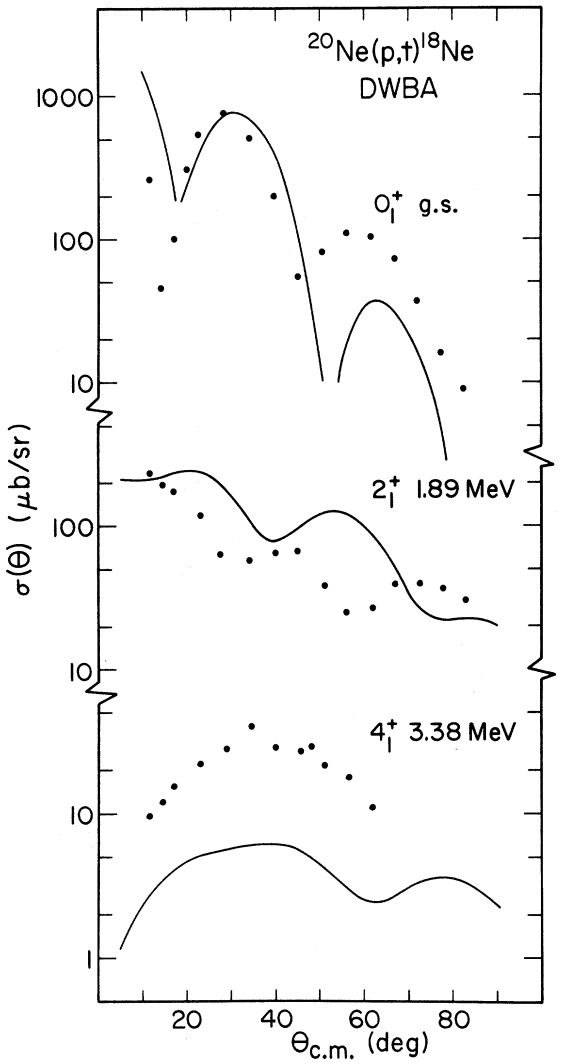

FIG. 2. Measured (p, t) cross sections (points) to the 0_1^+ ground state and to the 2_1^+ and 4_1^+ states in ^{18}Ne from 39.8-MeV proton bombardment of ^{20}Ne. The curves show the results of DWBA calculations with the optical-model potentials of Table III and with two-neutron spectroscopic amplitudes calculated from the wave functions of Refs. 3 and 4 using Eqs. (5) and (6). The calculated curves are normalized to the experimental data at the 30° maximum of the ground-state cross section.

III. ANALYSIS

A. Microscopic form factors

Two-neutron-transfer form factors were calculated from the mass-18 coexistence-model wave functions of Benson and Flowers[3,4] using the computer code TWOPAR.[20] This requires evaluation of two-neutron-transfer spectroscopic amplitudes

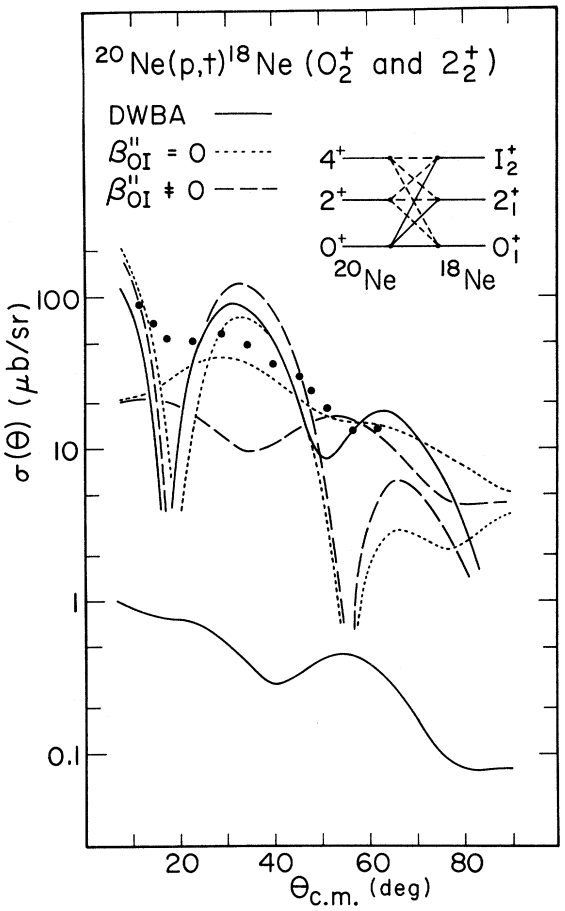

FIG. 3. Measured (p, t) cross section (points) to the $(0_2^+, 2_2^+)$ doublet in ^{18}Ne from 39.8-MeV proton bombardment of ^{20}Ne. The curves having pronounced maxima near 35° show the results of CCBA calculations for (p, t) transitions to the 0_2^+ state, and the flatter curves show the 2_2^+ calculated cross sections. The solid curves illustrate DWBA calculations, and the short-dashed and long-dashed curves show, respectively, CCBA cross sections in which the inelastic triton scattering has been described with two-quadrupole-phonon vibrational coupling schemes without ($\beta''_{0I} = 0.00$) one-phonon admixtures for these states and with ($\beta''_{00} = -0.08$ and $\beta''_{02} = 0.28$) one-phonon admixtures.

B defined by the matrix elements[21]

$$B(J_i; j_1 j_2 J; J_f) = (-1)^{J+J_i-J_f}\left[\frac{2J_i+1}{2J_f+1}\right]^{1/2} \langle \Psi^{J_i}(^{20}\mathrm{Ne})|\{D(1,2)[a^\dagger_{j_1}(n)a^\dagger_{j_2}(n)]^J \Psi^{J_f}(^{18}\mathrm{Ne})\}^{J_i}\rangle , \quad (1)$$

where the operator $a^\dagger_{j_1}(n)$ creates a neutron in the spherical single-particle state $(n_1 l_1 j_1)$, and

$$D(1,2) = (1+\delta_{n_1 n_2}\delta_{l_1 l_2}\delta_{j_1 j_2})^{-1/2} . \quad (2)$$

The ^{18}Ne wave functions[4] are of the form

$$\Psi^{J_f}_M(^{18}\mathrm{Ne}) = \sum_{j_1 \le j_2} X(j_1 j_2 J_f) D(1,2)[a^\dagger_{j_1}(p)a^\dagger_{j_2}(p)]^{J_f}_M|\,^{16}\mathrm{O}\rangle + \sum_{j_3 \le j_4} X(j_3 j_4 J_1 J_2 J_f) D(3,4)\{[a^\dagger_{j_3}(n)a^\dagger_{j_4}(n)]^{\dagger J_1}\Psi^{J_2}(^{20}\mathrm{Ne})\}^{J_f}_M , \quad (3)$$

where the configuration amplitudes X were determined by diagonalizing such states with a Kallio-Kolltveit interaction.[22] The first terms in Eq. (3) represent two protons moving in the $2s_{1/2}$, $1d_{3/2}$, and $1d_{5/2}$ orbits around a closed ^{16}O core, and the last terms represent two neutron holes moving in the $1p_{1/2}$ and $1p_{3/2}$ orbits coupled to J_1, in turn coupled to a four-particle state of angular momentum J_2, where these four-particle states are the members of the ^{20}Ne ground-state rotational band. The normalized wave functions for the ^{20}Ne ground-state $K^\pi = 0^+$ band were taken as[3,4]

$$\Psi^{J_i}_M(^{20}\mathrm{Ne}) = N(J_i)P^{J_i}_M \times[\alpha^\dagger_{1/2}(n)\alpha^\dagger_{-1/2}(n)\alpha^\dagger_{1/2}(p)\alpha^\dagger_{-1/2}(p)]|\,^{16}\mathrm{O}\rangle , \quad (4)$$

where $P^{J_i}_M$ is an angular momentum projection operator[23] and $N(J_i)$ is a normalization factor.[23] The operators $\alpha^\dagger_{\pm 1/2}$ create neutrons and protons in Nilsson orbit[24] No. 6 ($\Omega = \frac{1}{2}$) and are expanded in terms of $2s_{1/2}$, $1d_{3/2}$, and $1d_{5/2}$ spherical states with Nilsson transformation coefficients C_j, where $j = \frac{1}{2}, \frac{3}{2}$, and $\frac{5}{2}$. Benson and Flowers[3,4] determined these amplitudes to be $C_{1/2} = -0.40$, $C_{3/2} = -0.45$, and $C_{5/2} = 0.80$ by varying them to minimize the energy of the ground-state rotational band.

The matrix elements of Eq. (1) for transferring angular momentum J with two neutrons from orbits j_1 and j_2 were evaluated using the wave functions of Eqs. (3) and (4). The ^{18}Ne wave functions have both two-particle and four-particle–two-hole terms, and the resulting two-neutron-transfer spectroscopic amplitudes for the $2s_{1/2}$, $1d_{3/2}$, and $1d_{5/2}$ orbits have a different form from those for the $1p_{1/2}$ and $1p_{3/2}$ orbits. For the $1p_{1/2}$ and $1p_{3/2}$ orbits these amplitudes are simply given by

$$B(J_i; j_1 j_2 J; J_f) = X(j_1 j_2 J J_i J_f) , \quad (5)$$

where the configuration amplitudes $X(j_1 j_2 J J_i J_f)$ can be obtained directly from Table II of Ref. 4.

For the $2s_{1/2}$, $1d_{3/2}$, and $1d_{5/2}$ orbits, the matrix elements are more complicated and are given by the expression

$$B(J_i; j_1 j_2 J; J_f) = D(1,2)C_{j_1}C_{j_2}(-1)^{j_2-1/2}(j_1 \tfrac{1}{2} j_2 -\tfrac{1}{2}|\,J0)\,4N(J_i)(-1)^{J+J_i-J_f}\left(\frac{2J_i+1}{2J_f+1}\right)^{1/2}(J\,0\,J_f\,0|\,J_i\,0) \times \sum_{j_x \le j_y} C_{j_x}C_{j_y}(-1)^{j_y-1/2}(j_x \tfrac{1}{2} j_y -\tfrac{1}{2}|\,J0)X(j_x j_y J_f)D(x,y). \quad (6)$$

The matrix elements of Eq. (6) conveniently occur as the product of two factors, one of which is independent of the angular momenta J_i and J_f of the two states between which the two-neutron transfer occurs, and the other of which is independent of the angular momenta j_1 and j_2 of the particular s-d orbits from which the two neutrons are picked up. Therefore Eq. (6) can be written in the form

$$B(J_i; j_1 j_2 J; J_f) = B(0; j_1 j_2 J; J)P(J_i J_f J) , \quad (7)$$

which fact greatly simplifies the tabulation of the spectroscopic amplitudes. An index to distinguish between different states having the same J_f (e.g. the states 0^+_1 and 0^+_2) has been suppressed in our notation. The factor $B(0; j_1 j_2 J; J)$ of Eq. (7) has a simple physical interpretation; it is just the s-d two-neutron-transfer spectroscopic amplitude connecting the $J_i = 0^+$ ^{20}Ne ground state to the states $J_f (= J) = 0^+_1$, 2^+_1, and 4^+_1, of ^{18}Ne. These amplitudes are listed in Table I and, following Benson

TABLE I. Two-neutron spectroscopic amplitudes $B(0;j_1j_2J;J)$ for $2s_{1/2}$, $1d_{3/2}$, and $1d_{5/2}$ orbits for transitions from the $J_i=0^+$ ^{20}Ne ground state to the $J_f(=J)=0_1^+$, 2_1^+, and 4_1^+ states of ^{18}Ne.

J	n_1	l_1	$2j_1$	n_2	l_2	$2j_2$	$B(0;j_1j_2J;J)$
0_1^+	2	0	1	2	0	1	−0.1655
	1	2	3	1	2	3	−0.1481
	1	2	5	1	2	5	−0.3823
2_1^+	2	0	1	1	2	3	0.0795
	2	0	1	1	2	5	0.1413
	1	2	3	1	2	3	0.0447
	1	2	3	1	2	5	−0.0601
	1	2	5	1	2	5	0.1233
4_1^+	1	2	3	1	2	5	0.0560
	1	2	5	1	2	5	−0.0406

TABLE II. Factors $P(J_iJ_fJ)$ which, together with Table I and Eq. (7), determine the two-neutron spectroscopic amplitudes for all transitions for $2s_{1/2}$, $1d_{3/2}$, and $1d_{5/2}$ orbits.

J_i	J_f	J	$P(J_iJ_fJ)$	J_i	J_f	J	$P(J_iJ_fJ)$
0	0_2	0	−0.330	2	2_2	4	−0.603
0	2_2	2	−0.168	4	0_1	4	13.51
2	0_1	2	3.796	4	2_1	2	2.486
2	2_1	0	0.773	4	2_1	4	−4.640
2	2_1	2	−1.396	4	4_1	0	0.534
2	2_1	4	3.603	4	4_1	2	−0.902
2	4_1	2	0.699	4	4_1	4	1.867
2	4_1	4	−1.306	4	0_2	4	−4.450
2	0_2	2	−1.252	4	2_2	2	−0.416
2	2_1	0	−0.129	4	2_2	4	0.777
2	2_2	2	0.235				

and Flowers,[3,4] the tabulated values contain a factor 0.80 to allow for distortion of the ^{16}O core for the ^{20}Ne states. The factors $P(J_iJ_fJ)$ are listed in Table II, and, together with Table I and Eq. (7), allow construction of all the s-d spectroscopic amplitudes needed in the present calculation.

With these two-neutron spectroscopic amplitudes, form factors were calculated using the computer code TWOPAR,[20] which employ a zero-range interaction between the incoming proton and the di-neutron center of mass position. An rms matter radius of 1.67 fm was used for the triton.[25] The spherical single-particle bound-state wave functions of the transferred neutrons were generated in a Woods-Saxon potential with a radius of $1.25(20)^{1/3}$ fm, a diffuseness of 0.65 fm, and a spin-orbit potential of 30 times the Thomas term. The potential depth was adjusted for each single-particle state to give a binding energy equal to $\frac{1}{2}$ the two-neutron separation energy between the appropriate initial and final state. These form factors connect the coupled-channel waves in the entrance and exit channels.

B. Macroscopic coupled-channel waves

The present CCBA calculations use deformed optical potentials to generate coupled-channel distorted waves to describe the elastic and inelastic scattering in both the entrance and exit channels. These waves are calculated with the computer code JUPITOR-1.[26] This code requires optical potentials and deformation parameters, where the deformations usually describe either rotational or vibrational coupling.

The deformation parameters necessary for the $p+^{20}$Ne channel present no problem. The low-lying levels of ^{20}Ne can be accurately classified as members of well defined rotational bands.[27] In particular, the intrinsic quadrupole and hexadecapole deformations for the ground-state band have been determined to be $\beta_2=0.45$ and $\beta_4=0.25$, respectively, from coupled-channel analyses of proton elastic and inelastic scattering.[15,16] In addition, optical-model potentials for proton scattering are well understood. The parameters for the proton potential we use are listed in Table III and were obtained from a global analysis of proton scattering from $1p$-shell nuclei.[28] Although this charge, mass, and energy dependent potential was obtained from $1p$-shell nuclei, it is very similar to potentials obtained from coupled-channel analyses of cross section and polarization data for proton elastic and inelastic scattering near 25 MeV from target nuclei in the lower half of the $2s$-$1d$ shell.[15,17,29]

The optical potential and deformation parameters necessary for the $t+^{18}$Ne channel present a problem, however. In principle we require coupled-channel parameters for 20.9-MeV triton elastic

TABLE III. Optical-model parameters.

Channel	r_R (fm)	a_R (fm)	V_R (MeV)	r_I (fm)	a_I (fm)	W_V (MeV)	W_D (MeV)	r_c (fm)
p	1.11	0.57	51.1	1.11	0.50	6.0	7.3	1.11
t	1.08	0.73	177.1	1.73	0.80	17.4	0.0	1.40

and inelastic scattering from ^{18}Ne, which of course are unavailable. Hence, we use the optical potential of Oh *et al.*,[30] which was obtained from 22.4-MeV ^{3}He scattering on ^{19}F. The parameters of this potential are given in Table III and give slightly better fits to the present (p,t) data than do the global triton parameters of Becchetti and Greenlees,[31] which were used in a previous[12] CCBA analysis of the ^{22}Ne$(p,t)^{20}$Ne reaction.

There has been considerable speculation on the nature of the low-lying levels of ^{18}O (or, equivalently, the mirror nucleus ^{18}Ne). The wave functions used here[3,4] allow both two-particle (spherical) and four-particle-two-hole (deformed) components. The deformed components correspond[3,4] to permanent deformations of $\beta_2 = 0.39$ and $\beta_4 = 0.17$, and, although the two-particle components are generated in a spherical potential, they nevertheless contribute to the mass moments. We attempt to obtain some information on the ^{18}Ne states involved in our (p,t) calculations by considering the 24.5-MeV $p + ^{18}$O inelastic scattering data of the Saclay group.[17] They measured cross sections and polarizations for proton scattering to many low-lying levels of ^{18}O and reported a good fit to the elastic, 2_1^+ (1.98-MeV), and 4_2^+ (7.11-MeV) data treated as a rotational band in a coupled-channel analysis. Although they emphasized the polarization data, we here ignore the polarization data, because we do not include spin-orbit forces in our CCBA calculations. Employing their[17] optical potential, we have used JUPITOR-1 to fit their cross sections in order to estimate deformation parameters in a manner consistent with their use in our CCBA calculation. Our fits to their[17] data are not shown here, but the deformations resulting from this analysis are listed in Table IV and require some explanation.

Because it is not at all obvious which coupling scheme is appropriate, calculations were performed to fit the Saclay[17] cross sections with both rotational and vibrational coupling for the ^{18}O states. With either coupling scheme, almost identically good fits were obtained to the elastic, 2_1^+, and 4_1^+ cross sections. When we used only a 0_1^+-2_1^+ coupling, the resulting quadrupole deformation for a rotation ($\beta_2 = 0.40$) was slightly smaller than that for a vibration ($\beta_{02} = 0.42$). Moreover, when the 4_1^+ state was added to the ^{18}O coupling, the resulting quadrupole and hexadecapole deformations for a rotation ($\beta_2 = 0.36$ and $\beta_4 = 0.29$) were smaller than the corresponding quantities for a vibration ($\beta_{02} = 0.42$, $\beta''_{04} = 0.31$). The deformation β''_{04} is a measure of the one-phonon admixture in the "two-phonon" state.[32] In all the above cases the fits to the experimental angular distributions were good, and one could not distinguish whether the 0_1^+-2_1^+-4_1^+ sequence was rotational or vibrational. Hence we consider both types of coupling in our (p,t) analysis.

TABLE IV. Coupled-channel deformation parameters to excited states of $T=1$ mass-18 states. The parameters were determined from an analysis of 24.5-MeV proton scattering by ^{18}O.

Coupling	β_2 or β_{02}	β_4 or β''_{0I}
Rot. 0_1^+-2_1^+	0.40	···
Rot. 0_1^+-2_1^+-4_1^+	0.36	0.29
Vib. 0_1^+-2_1^+	0.42	···
Vib. [a] 0_1^+-2_1^+-4_1^+	0.42	0.31
Vib. [a] 0_1^+-2_1^+-0_2^+	0.42	−0.08
Vib. [a] 0_1^+-2_1^+-2_2^+	0.42	0.28

[a] $\beta'_{0I} = \beta_{2I} = \beta_{02}$.

The inelastic cross sections to the 0_2^+ and 2_2^+ states could not be reproduced well either by interpreting them as two-quadrupole-phonon vibrations with one-phonon admixtures (as with the 4_1^+ state) or as a β band. However, the fits were best when these states were treated as "two-phonon" vibrations, and the corresponding deformations ($\beta''_{00} = -0.08$ and $\beta''_{02} = 0.28$) were used in our CCBA (p,t) calculations. Most of the inelastic strength to all three of the "two-phonon" states comes mainly from their one-phonon admixtures.

C. Comparison with experiment

With the form factors, optical potentials, and deformations described in the previous two subsections, DWBA and CCBA cross sections were calculated with the computer code MARS.[33] DWBA results for the 0_1^+, 2_1^+, and 4_1^+ cross sections are represented by the curves in Fig. 2, and these calculations are normalized to the experimental data at the 30° maximum of the 0_1^+ ground-state transition. The shape of the DWBA calculation for the ground-state transition is similar to the data; however the calculation is nearly 5° out of phase with the data and it markedly underestimates the strength of the second maximum. The calculated relative cross section for the 2_1^+ state is too large and is completely out of phase with the experimental results, and the calculated relative cross section for the 4_1^+ state has approximately the correct shape, but its strength is five times smaller than required by the data.

Figures 3–6 show how the calculated CCBA cross sections with various ^{18}Ne rotational and vibrational coupling schemes compare with the experimental data. In these calculations we always employ a 0^+-2^+-4^+ rotational coupling for

^{20}Ne with $\beta_2 = 0.45$ and $\beta_4 = 0.25$. Specifically, Fig. 4 shows CCBA results for a 0_1^+-2_1^+ coupling in ^{18}Ne with the deformations given in Table IV. The solid curve is for $\beta_{02} = 0.42$ with a ^{18}Ne 2_1^+ mass-quadrupole moment Q of zero, which corresponds to vibrational coupling; the short-dashed curve is for rotational coupling ($\beta_2 = 0.40$), where of course the ^{18}Ne mass quadrupole moment is equal to the rotational value Q_R; and the long-dashed curve is for an intermediate case ($\beta_{02} = 0.41$) where the mass quadrupole moment was set equal to $\frac{1}{2}$ the rotational value. It is seen that the inclusion of inelastic excitations dramatically improves both the shape and relative strength of the 2_1^+ cross section. Furthermore, the fit to the shape of the 0_1^+ cross section is definitely improved. Unfortunately, however, the magnitude of the 2_1^+ cross section depends on the ^{18}Ne 2_1^+ mass quadrupole moment, which is unknown. In particular, the (p,t) cross sections are more sensitive to the type of coupling than are the 24.5-MeV proton inelastic scattering cross sections; all three values of the mass quadrupole moment Q used in Fig. 4 give equally good fits to the $p+^{18}O$ inelastic scattering data. Of course this need not be the case for $t+^{18}Ne$ scattering.

When the 4_1^+ state is included in the coupling

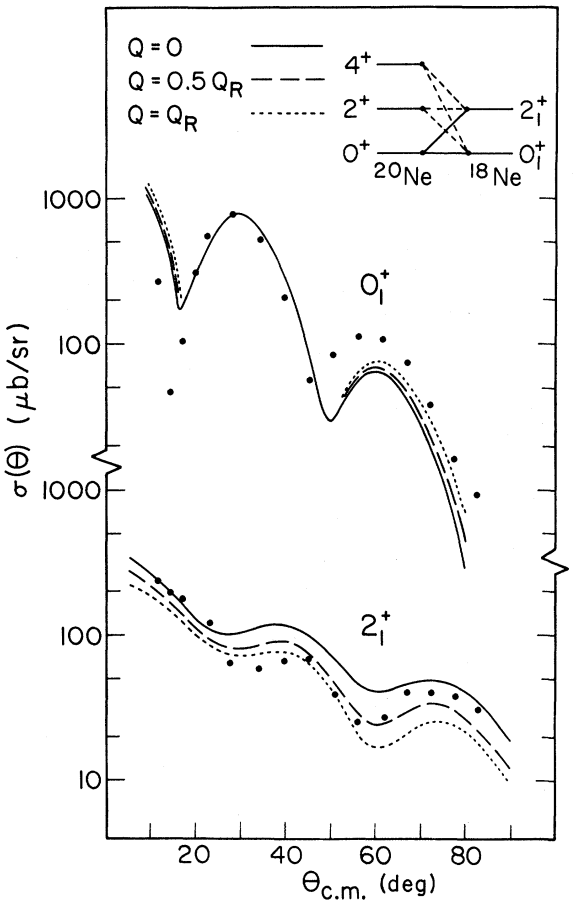

FIG. 4. Measured (p,t) cross sections (points) to the 0_1^+ ground state and to the 2_1^+ state in ^{18}Ne from 39.8-MeV bombardment of ^{20}Ne. The coupling scheme is illustrated in the figure. The solid, long-dashed, and short-dashed curves show, respectively, the results of CCBA calculations using a mass quadrupole moment of zero with $\beta_{02} = 0.42$, a mass quadrupole moment of one-half the rotational value with $\beta_{02} = 0.41$, and a mass quadrupole moment of the full rotational value with $\beta_2 = 0.40$.

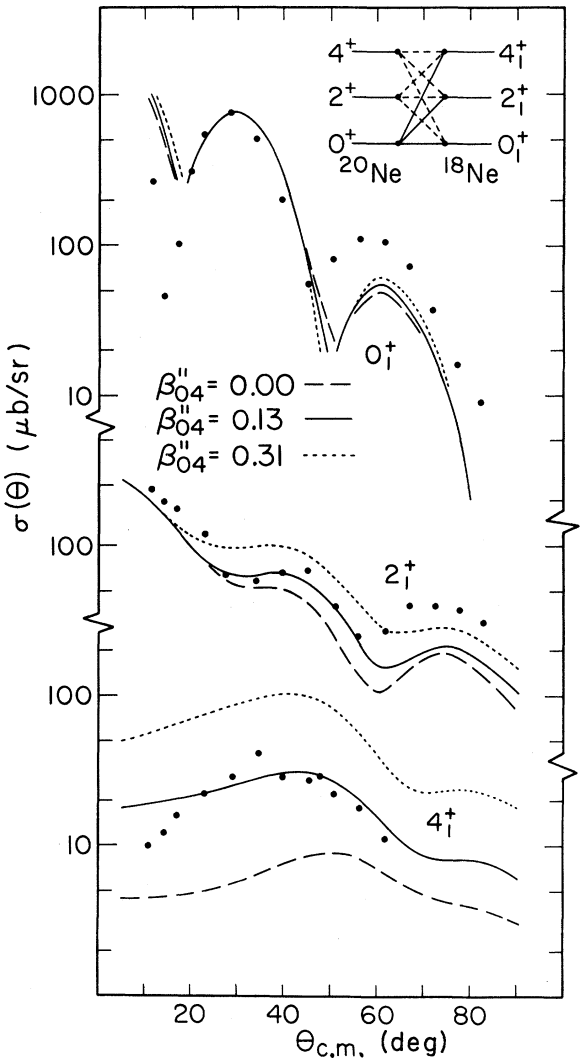

FIG. 5. Measured (p,t) cross sections (points) to the 0_1^+ ground state and to the 2_1^+ and 4_1^+ states in ^{18}Ne from 39.8-MeV proton bombardment of ^{20}Ne. With vibrational coupling for ^{18}Ne, the short-dashed, solid, and long-dashed curves show the results of CCBA calculations with $\beta_{04}'' = 0.31$, 0.13, and 0.00, respectively. The strength of the (p,t) transition to the 4_1^+ state is very sensitive to β_{04}'' and is fit best with $\beta_{04}'' = 0.13$.

scheme for $t+^{18}$Ne inelastic scattering, the (p,t) calculations are even more sensitive to the description of this scattering. Figures 5 and 6 show CCBA cross sections for 0_1^+-2_1^+-4_1^+ vibrational and rotational couplings, respectively. The short-dashed curves in Fig. 5 represent calculations using the deformations of Table IV, and it is seen that they give too much 4_1^+ strength. The solid and long-dashed curves in Fig. 5 represent calculations with $\beta''_{04}=0.13$ and 0.00, respectively, and illustrate that the relative (p,t) cross section to the 4_1^+ state increases very strongly with the inelastic strength to the ^{18}Ne 4_1^+ state. In particular, the experimental (p,t) relative 4_1^+ strength is reproduced with $\beta''_{04}=0.13$, whereas the proton data[17] require $\beta''_{04}=0.31$. Perhaps this is not too surprising because it is known[34] that heavier projectiles give smaller deformations for a given state than do lighter projectiles, particularly for high-multipole excitations of light nuclei. In addition, the smaller β''_{04} value gives a better fit to the 2_1^+ cross section. Figure 6 shows similar calculations with rotational coupling for the ^{18}Ne scattering. Again the relative (p,t) strength to the 4_1^+ state requires a reduction of the value of the hexadecapole deformation determined from proton inelastic scattering; however, the rotational coupling scheme for ^{18}Ne appears to provide too much destructive interference for the 2_1^+ transition, thereby reducing its strength to $\frac{1}{2}$ of the experimental value. Clearly, vibrational coupling with $\beta''_{04}=0.13$ gives the most reasonable reproduction of the experimental data.

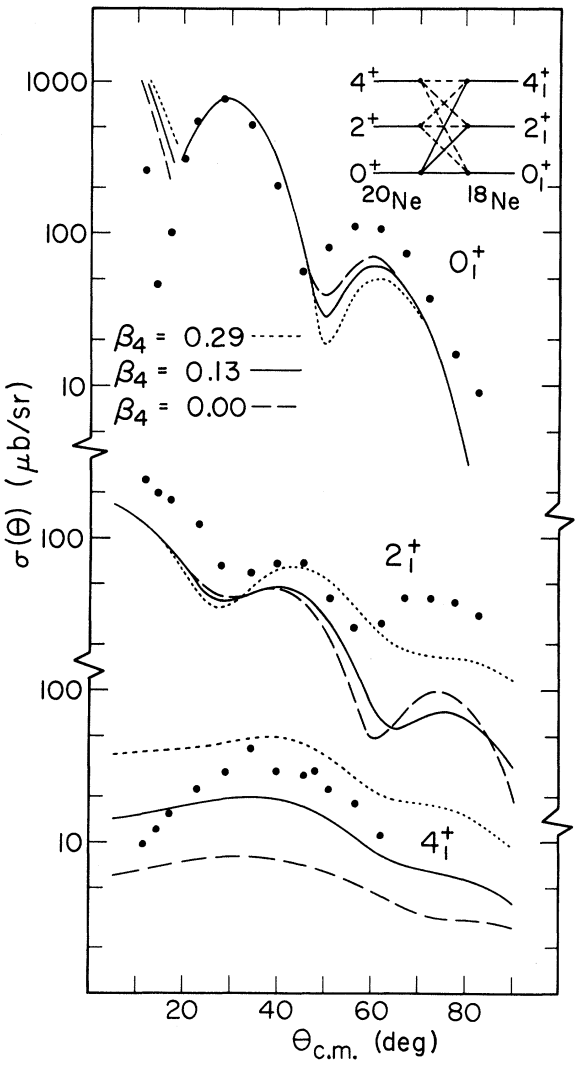

FIG. 6. Measured (p,t) cross sections (points) to the 0_1^+ ground state and to the 2_1^+ and 4_1^+ states in ^{18}Ne from 39.8-MeV proton bombardment of ^{20}Ne. With rotational coupling for ^{18}Ne, the short-dashed, solid, and long-dashed curves show results of CCBA calculations for $\beta_4=0.29$, 0.13, and 0.00, respectively.

Although we did not experimentally resolve the cross sections to the 0_2^+ and 2_2^+ states, calculations of these cross sections are also of interest and are illustrated in Fig. 3. There are shown three calculated cross sections for (p,t) transitions to both the 0_2^+ and 2_2^+ state. The 0_2^+ calculated cross sections are represented by the curves having pronounced maxima near 35°, and the flatter curves show the 2_2^+ calculated cross sections. The solid curves show the DWBA results, the long-dashed curves show the CCBA results using the ^{18}Ne couplings given in the bottom two entries of Table IV, and the short-dashed curves show CCBA results assuming the 0_2^+ and 2_2^+ states are pure two-phonon vibrations with no one-phonon components ($\beta''_{01}=0$). The sum of the cross sections to the 0_2^+ and 2_2^+ states is what is to be compared with the experimental points in Fig. 3. Curves representing these calculated sums are not shown in this figure; however, it is clear that the calculations yield too much (p,t) strength to the 0_2^+ state. Because the shape and the relative strength of the calculated cross section to the 0_2^+ state are not drastically altered by changes in the coupling scheme (see Fig. 3) we tentatively ascribe this discrepancy to deficiencies in the wave functions used.[3,4]

IV. CONCLUSIONS

Differential cross sections for (p,t) transitions produced by 39.8-MeV proton bombardment of ^{20}Ne have been measured for transitions to the ground, 2_1^+, and 4_1^+ states and $(0_2^+, 2_2^+)$ doublet in ^{18}Ne. These cross sections are in reasonable agreement with those reported by others.[6-9] We have compared our cross sections with zero-range CCBA

calculations employing the coexistence-model wave functions of Benson and Flowers.[3,4] In general, the effects of the inelastic excitations are very large. This fact makes the comparison difficult, because the proper description of triton inelastic scattering by ^{18}Ne is not known. Nevertheless, by considering a variety of ^{18}Ne coupling schemes with deformation parameters determined from 24.5-MeV proton inelastic scattering[17] by ^{18}O, the following conclusions can be made.

The inclusion of inelastic effects causes a drastic improvement over the DWBA in the shape of the calculated 2_1^+ cross section. Such an improvement in 2_1^+ cross sections has always been observed to occur in CCBA calculations. In addition, the inclusion of inelastic effects greatly increases the calculated relative 4_1^+ strength over that given by the DWBA, thereby bringing the calculation into much better agreement with experiment. Both the shape and magnitude of the CCBA cross section to the 0_2^+ state is rather stable against changes in the description of $t+^{18}$Ne inelastic scattering. This fact has led us to suggest that the reason the CCBA calculation gives too large a (p,t) cross section to the 0_2^+ state is that the wave function[3,4] used for this state is somehow deficient. It would certainly be of interest to resolve experimentally the (p,t) cross sections to the 0_2^+ and 2_2^+ states in order to allow a more definitive comparison. Finally, a coupled-channel analysis of α-particle, ^{3}He, or t inelastic scattering cross sections to the appropriate states in ^{18}O would remove many of the ambiguities in the present calculations.

ACKNOWLEDGMENTS

We wish to thank Professor B. F. Bayman for making the computer code TWOPAR available to us and to thank the entire technical staff of the John H. Williams Laboratory of Nuclear Physics for their help in the experimental aspects of this work. The assistance of D. Madland in the data taking is gratefully acknowledged. J. L. Escudie, R. Lombard, M. Pignanelli, F. Resmini, and A. Tarrats are thanked for sending us their cross sections for proton inelastic scattering by ^{18}O.

---

*Work supported in part by the U.S. Atomic Energy Commission. Contracts No. AT-(11-1)-1265 and No. AT-(40-1)-2972.

†Present address: Oak Ridge National Laboratory, Oak Ridge, Tennessee 37830.

[1]F. Ajzenberg-Selove, Nucl. Phys. A190, 1 (1972).

[2]J. B. McGrory and B. H. Wildenthal, Phys. Rev. C 7, 974 (1973); G. E. Brown, in *Proceedings of the International Conference on Nuclear Physics, Paris, France, 1964,* edited by P. Gugenberger (Centre National de la Recherche Scientifique, Paris, France, 1964), Vol. 1, p. 129; H. G. Benson and J. M. Irvine, Proc. Phys. Soc. (Lond) 89, 249 (1966); P. Federman, Nucl. Phys. A95, 443 (1967); P. Federman and I. Talmi, Phys. Lett. 19, 490 (1965); T. Engeland, Nucl. Phys. 72, 68 (1965); P. J. Ellis and T. Engeland, *ibid.* A144, 161 (1970); A. P. Zuker, Phys. Rev. Lett. 23, 983 (1969).

[3]H. G. Benson and B. H. Flowers, Nucl. Phys. A126, 305 (1969).

[4]H. G. Benson and B. H. Flowers, Nucl. Phys. A126, 332 (1969).

[5]F. Dönau, K. Hehl, C. Riedel, R. A. Broglia, and P. Federman, Nucl. Phys. A101, 495 (1967).

[6]W. R. Falk, R. J. Kidney, P. Kulisic, and G. K. Tandon, Nucl. Phys. A157, 241 (1970).

[7]J. L'Ecuyer, R. D. Gill, K. Ramavataram, N. S. Chant, and D. G. Montague, Phys. Rev. C 2, 116 (1970).

[8]R. A. Paddock, Phys. Rev. C 5, 485 (1972).

[9]J. C. Hardy, H. Brunnader, J. Cerny, and J. Jänecke, Phys. Rev. 183, 854 (1969).

[10]S. K. Penny and G. R. Satchler, Nucl. Phys. 53, 145 (1964).

[11]T. Tamura, D. R. Bes, R. A. Broglia, and S. Landowne, Phys. Rev. Lett. 25, 1507 (1970); 26, 156(E) (1971); R. J. Ascuitto, N. K. Glendenning, and B. Sorensen, Phys. Lett. 34B, 17 (1971); Nucl. Phys. A183, 60 (1972).

[12]D. K. Olsen, T. Udagawa, T. Tamura, and R. E. Brown, Phys. Rev. Lett. 29, 1178 (1972); Phys. Rev. C 8, 609 (1973); in *Proceedings of the International Conference on Nuclear Physics, Munich, August, 1973,* edited by J. de Boer and H. J. Mang (North-Holland, Amsterdam/American Elsevier, New York, 1973), Vol. 1, p. 489; T. Udagawa and D. K. Olsen, Phys. Lett. 46B, 285 (1973).

[13]R. J. Ascuitto and N. K. Glendenning, Phys. Rev. C 2, 415, 1260 (1970); T. Udagawa, T. Tamura, and T. Izumoto, Phys. Lett. 35B, 129 (1971); T. Udagawa, Phys. Rev. C 9, 270 (1974).

[14]D. K. Olsen, T. Udagawa, and R. E. Brown, Bull. Am. Phys. Soc. 18, 1400 (1973).

[15]R. de Swiniarski, A. Genoux-Lubain, G. Bagieu, J. F. Cavaignac, and D. H. Worledge, Phys. Lett. 43B, 27 (1973); R. de Swiniarski, A. D. Bacher, F. G. Resmini, G. R. Plattner, D. L. Hendrie, and J. Raynal, Phys. Rev. Lett. 28, 1139 (1972).

[16]D. Madland, Ph.D. thesis, University of Minnesota, 1970 (unpublished).

[17]F. Resmini, R. M. Lombard, M. Pignanelli, J. L. Escudie, and A. Tarrats, Phys. Lett. 37B, 275 (1971).

[18]J. Stevens, H. F. Lutz, and S. F. Eccles, Nucl. Phys. 76, 129 (1966); H. F. Lutz and S. F. Eccles, *ibid.* 81,

423 (1966).
[19]D. K. Olsen, Ph.D. thesis, University of Minnesota, 1970 (unpublished); D. K. Olsen and R. E. Brown, Nucl. Phys. A170, 544 (1971).
[20]B. F. Bayman and A. Kallio, Phys. Rev. 156, 1121 (1967); B. Bayman, private communication.
[21]The following phase conventions are used, (i) spherical harmonics have Condon-Shortly phases; (ii) $\vec{l}+\vec{s}=\vec{j}$ instead of $\vec{s}+\vec{l}=\vec{j}$; (iii) radial wave functions start off positive at the origin independent of l. We should also mention that the phases of the wave functions of Ref. 3 and 4 have been adjusted to be consistent with the requirements of the formalism used in the coupled-channel code JUPITOR-1 (Ref. 26). This was done by calculating the $E2$ and $E4$ matrix elements connecting the ^{18}Ne states of interest and by requiring that the phases of the wave functions for these states be such that the sign of each electric matrix element be the same as that of the corresponding β parameter in Table IV.
[22]A. Kallio and K. Kolltveit, Nucl. Phys. 53, 87 (1964).
[23]I. Unna, Phys. Rev. 132, 2225 (1963).
[24]S. G. Nilsson, K. Dan. Vidensk. Selsk. Mat.—Fys. Medd. 29, No. 16 (1955).
[25]This is close to the value of 1.63 fm extracted from the triton charge radius. See Table I and Appendix A of J. A. Koepke, R. E. Brown, Y. C. Tang, and D. R. Thompson, Phys. Rev. C 9, 823 (1974).
[26]T. Tamura, Rev. Mod. Phys. 37, 679 (1965); Oak Ridge National Laboratory Report No. ORNL-4152, 1967 (unpublished).
[27]O. Häusser, T. K. Alexander, A. B. McDonald, G. T. Ewan, and A. E. Litherland, Nucl. Phys. A168, 17 (1971).
[28]B. A. Watson, P. P. Singh, and R. E. Segel, Phys. Rev. 182, 977 (1969).
[29]R. M. Lombard and J. Raynal, Phys. Rev. Lett. 31, 1015 (1973); R. de Swiniarski, H. E. Conzett, B. Frois, R. Lamontagne, R. J. Slobodrian, Lawrence Berkeley Laboratory Nuclear Chemistry Annual Report No. LBL-1234, 1973 (unpublished).
[30]I. K. Oh, C. S. Zaidins, C. D. Zafiratos, and S. I. Hayakawa, Nucl. Phys. A178, 497 (1972).
[31]F. D. Becchetti, Jr., and G. W. Greenlees, in *Proceedings of the Third International Symposium on Polarization Phenomena in Nuclear Reactions*, edited by H. H. Barschall and W. Haeberli (University of Wisconsin Press, Madison, Wisconsin, 1971), p. 682.
[32]See Ref. 26 for definitions of the β parameters. It is also mentioned in Ref. 26 that the introduction of explicit coupling to excited states requires reductions in the strength of the optical-model imaginary potential determined from elastic scattering. With both rotational and vibrational, mass-18 0_1^+-2_1^+ coupling the triton elastic imaginary potential was reduced by 10% from the value in Table III. With vibrational 0_1^+-2_1^+-I_2^+ coupling the triton imaginary potential was reduced by 15% and 5%, respectively, for the ground and 2_1^+ states, whereas with 0_1^+-2_1^+-4_1^+ rotational coupling the triton imaginary potential was reduced by 15% for the ground state only. The proton imaginary potential was not reduced.
[33]T. Tamura and T. Udagawa, Center for Nuclear Studies, University of Texas, Technical Report No. 30, 1972 (unpublished); A. K. Abdallah, T. Udagawa, and T. Tamura, Phys. Rev. C 8, 1885 (1973).
[34]For example: D. L. Hendrie, Phys. Rev. Lett. 31, 478 (1973); H. Rebel, G. W. Schweimer, G. Schatz, J. Specht, R. Löhken, G. Hauser, D. Habs, and H. Klewe-Nebenius, Nucl. Phys. A182, 145 (1972).